Tormentas cálidas en Chile central

René D. Garreaud
Departamento de Geofísica
Universidad de Chile

14 de Septiembre 2012 – Seminarios CIMA-DAO UBA

Agradecimientos: Fondecyt 1110169, José Rutllant, Robert Rondanelli

Temario

- Revisión de trabajos previos
- Datos (Diarios DMC; 15’ DGF; CFSR; TMI/SMI…)
- Variabilidad de la línea de nieves e impactos hidro.
- Tormentas cálidas y frías
- Caso de estudio (Julio 2006)
- Análisis compuesto
- Modelo conceptual y conclusiones

Geographical setting…

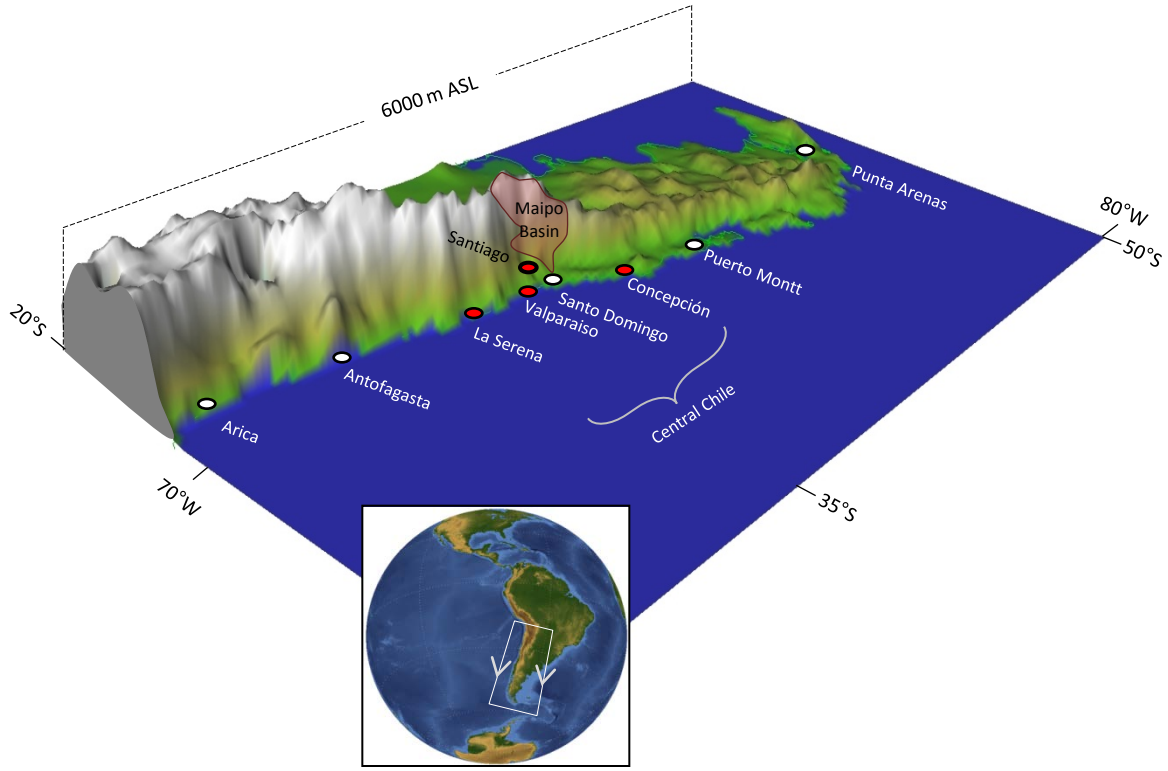

Rutllant and Fuenzalida 1991: Synoptic explanation of increased CCh precipitation during EN years: blocking anticyclone shifts northward storm track and embedded frontal systems

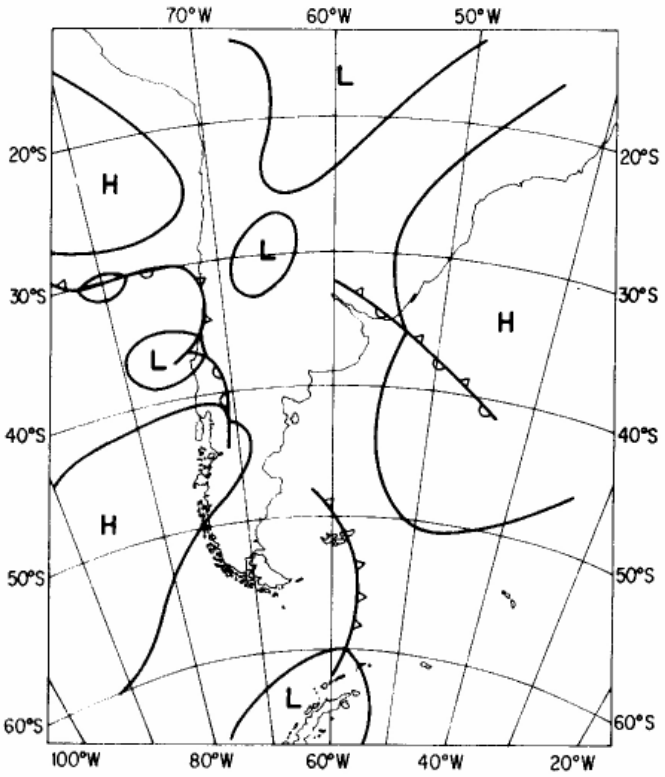

Figure 3. Composite SLP chart with the most frequent features associated with rainfall events in 1972 and 1982 (from Rutllant, 1987)

Viale and Nuñez 2011: NNR Composite fields of CCh precipitation events.
Extreme events exhibit sharper / more intense features than intense events.

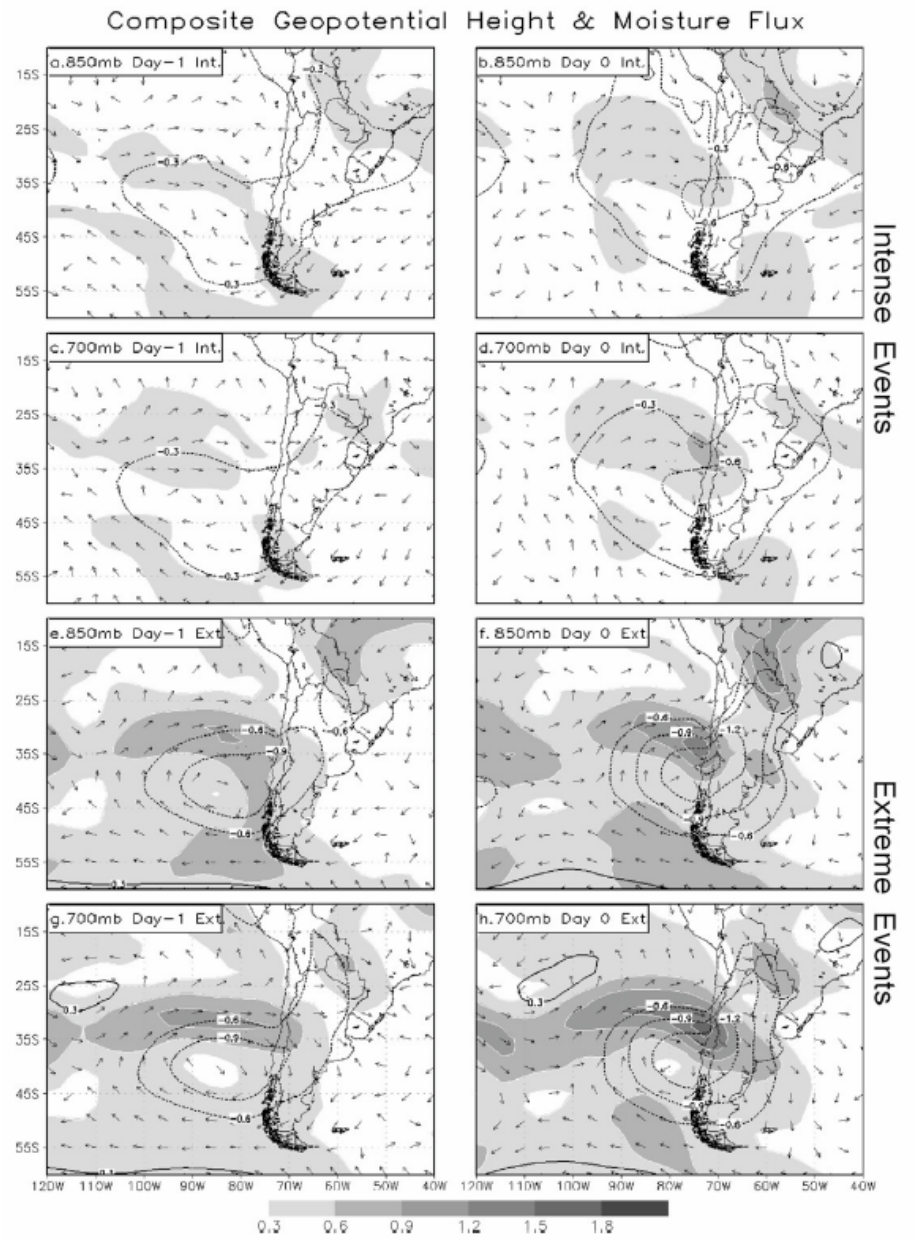

Viale and Nuñez 2011: Extreme events more often associated with an atmospheric river.

Extreme

Intense

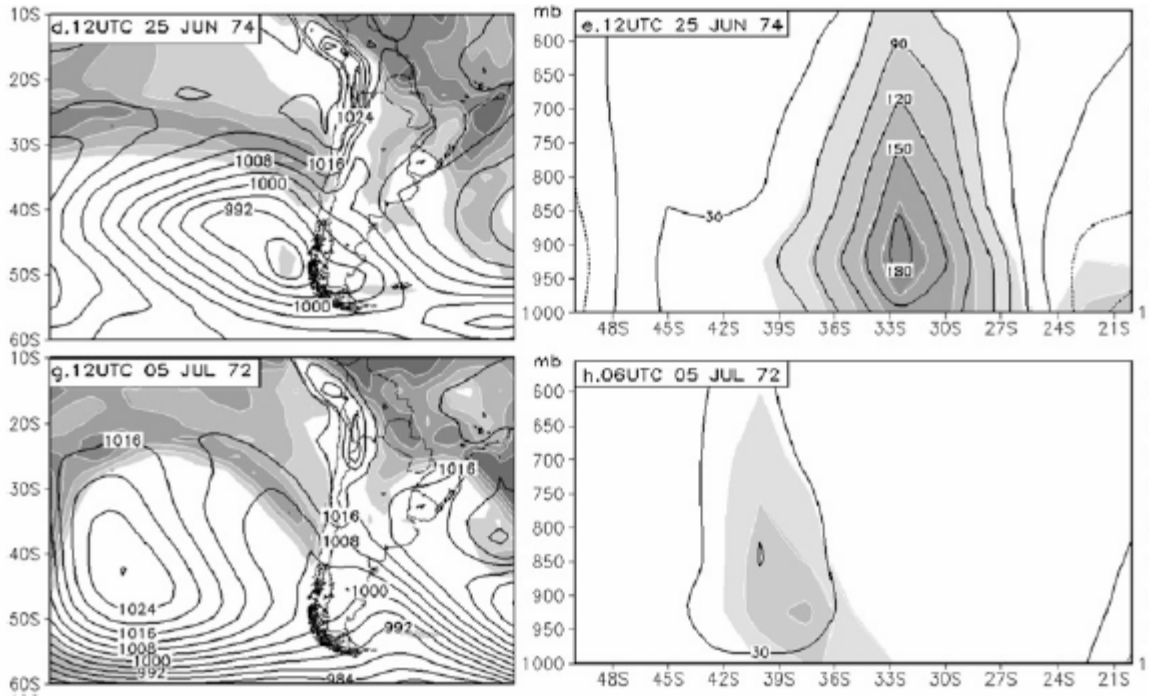

Barret et al. 2012: Composite fields (QS sfc. Wind, TRMM, Z500, etc.) of CCh precipitation events. More amplified/slower systems cause more precipitation

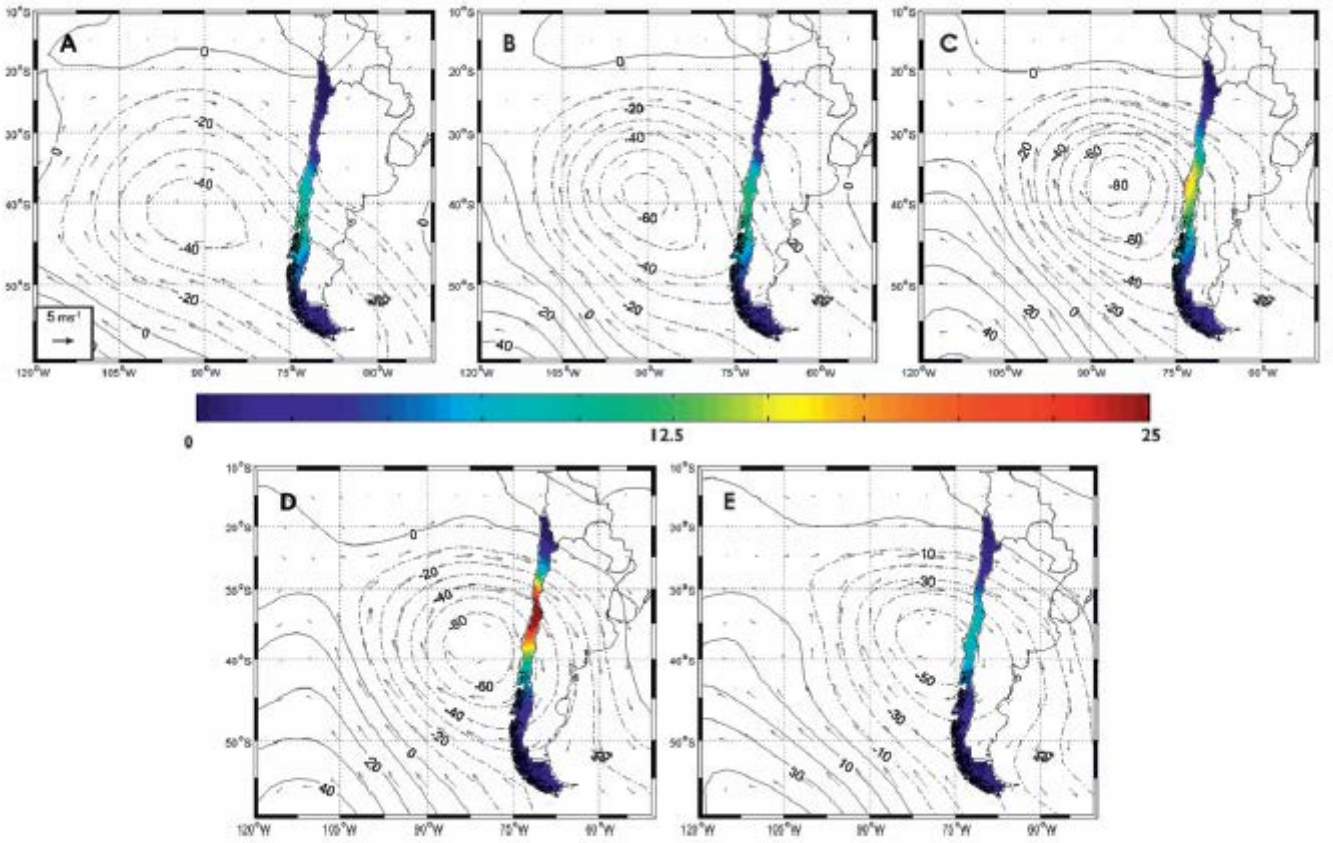

FIG. 10. As in Fig. 8, but for 500-hPa height and wind anomalies associated with a PE rainfall threshold of 25 mm.

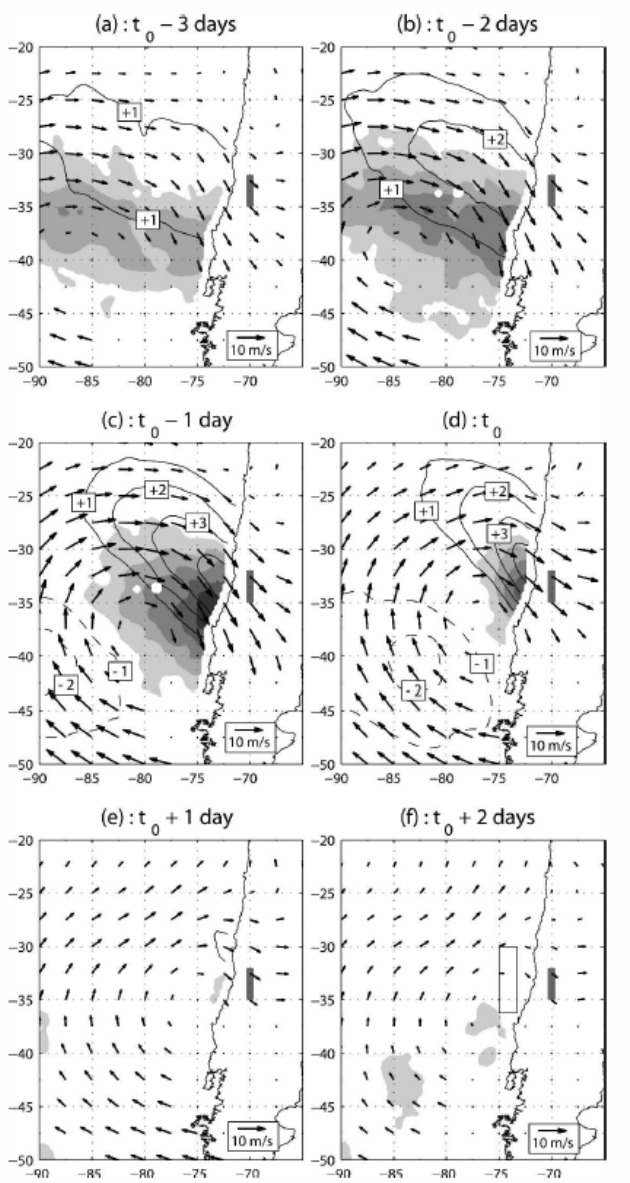

Falvey & Garreaud 2007: Composite fields and Radiosonde profiles (local conditions) of CCh precipitation events.

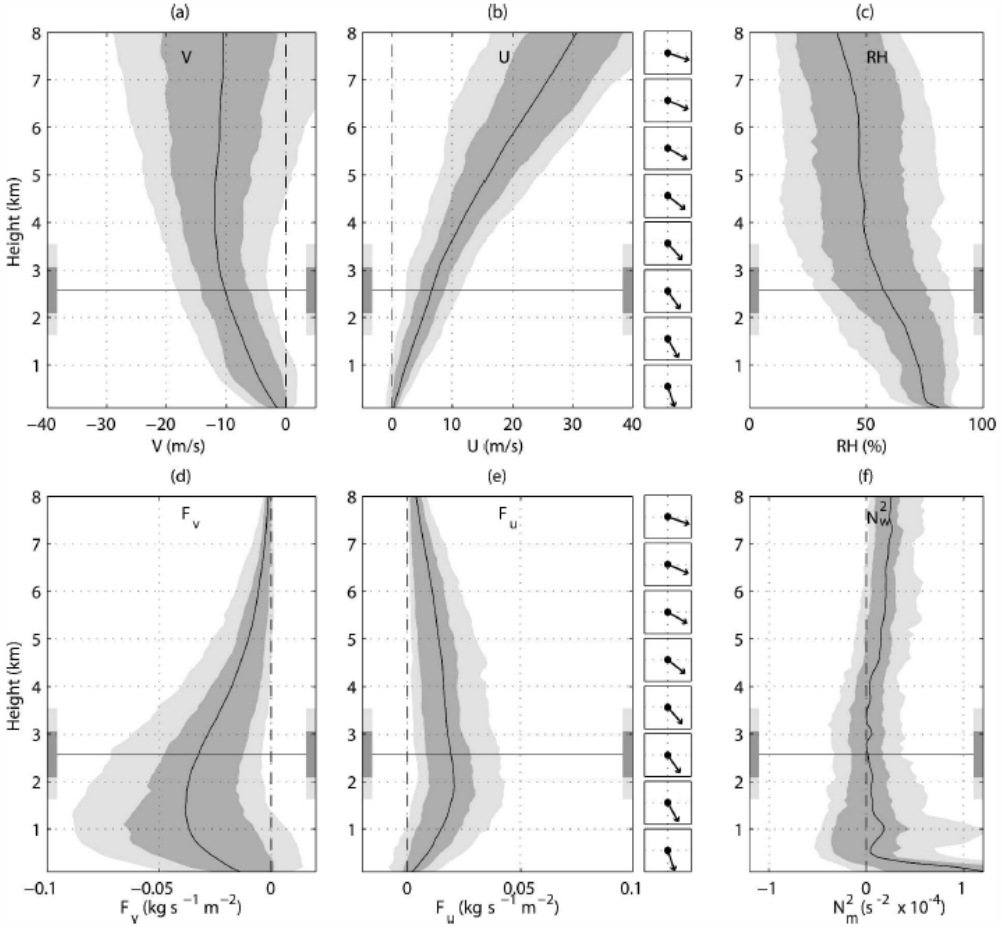

Falvey & Garreaud 2007. They also shown a statistically robust correlation between CCh rainfall and low-level zonal moisture transport

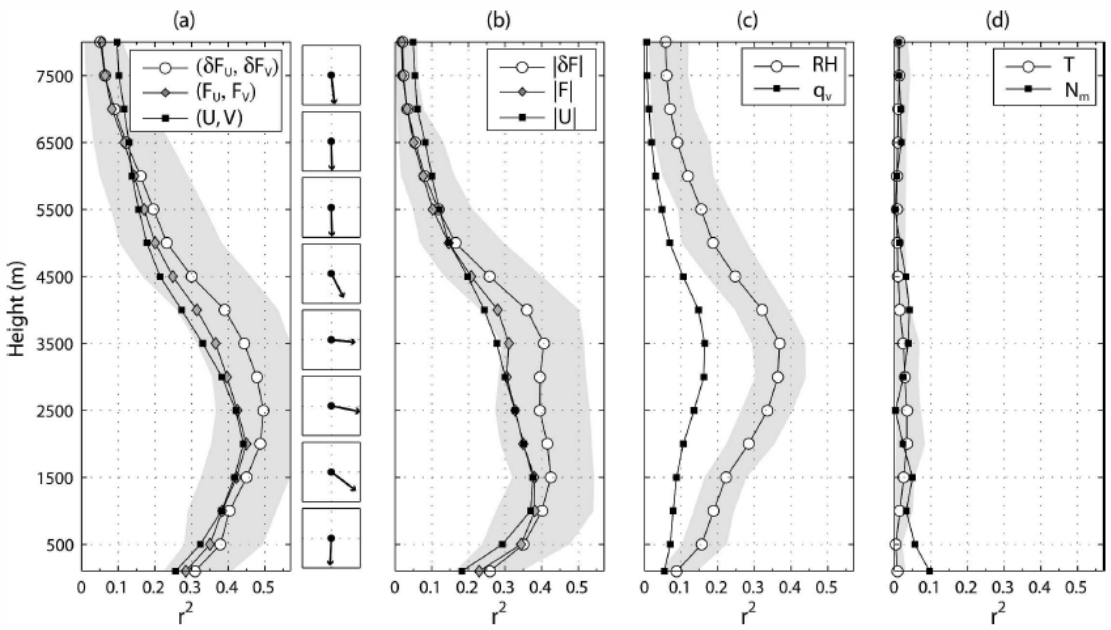

FIG. 7. Results of a linear fit between P_m and variables derived from the coastal radiosonde. The goodness of fit is measured by the r^2 statistic and is plotted as a function of height for each of the parameters tested. The gray region shows the 95% confidence region of r^2 for the predictors corresponding to the white circle symbols. The arrows to the right of (a) indicate the direction of the component of the flux vector (δF_U, δF_V) that gives the best fit to P_m.

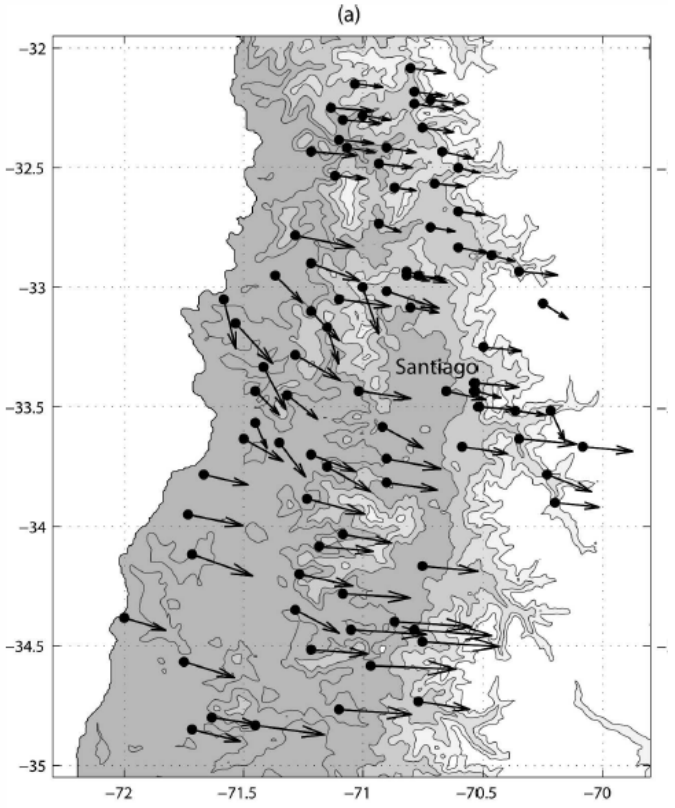

FIG. 9. (a) Results of the regression of the humidity-weighted moisture flux vector (δF_U, δF_V) against precipitation at individual rain gauges. The length of the arrows in (a) indicates r^2 at its level of maximum value, and their orientation indicates the direction of the component of the flux vector (δF_U, δF_V) that gives the best fit to the precipitation. (b) The statistic r^2 as a function of latitude and (c) the height where the r^2 is greatest.

Garreaud et al. 2012. Using PRECIS-ERA40 data, they show that strong (local) correlation between 850 hPa zonal wind and precipitation extends along south-central Chile because of the orographic enhancement in the windward side of the Andes

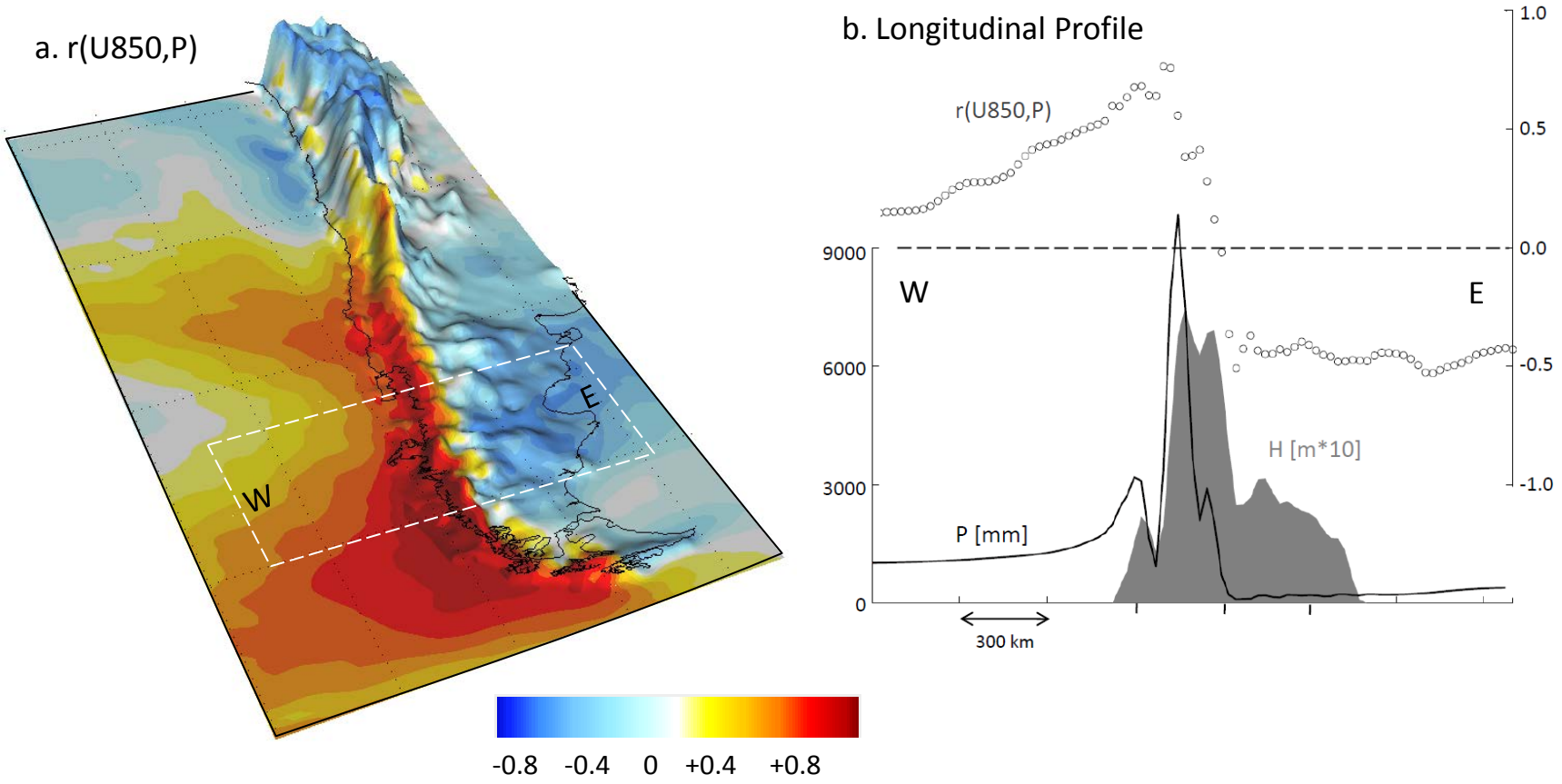

Hydrological Impacts

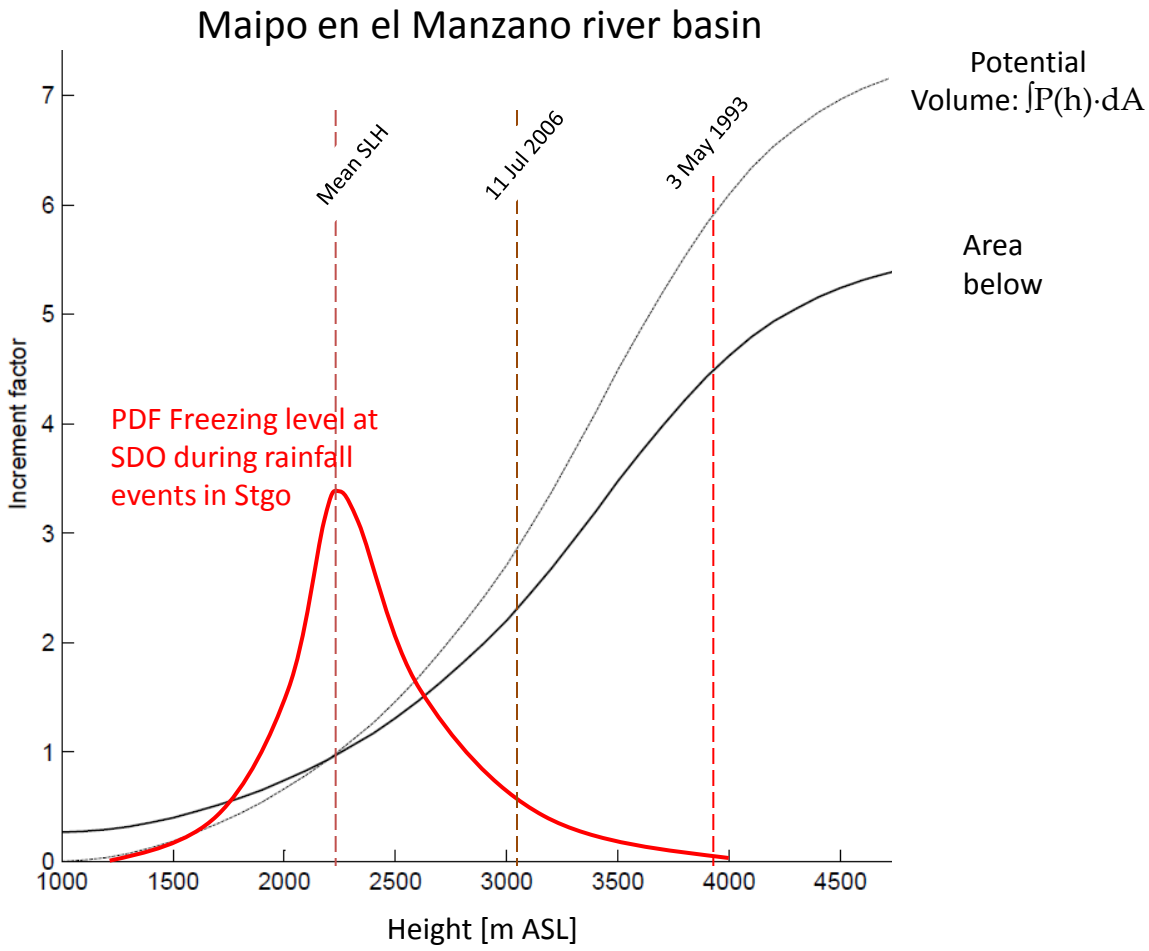

Freezing level variability during winter storms (MJJAS)

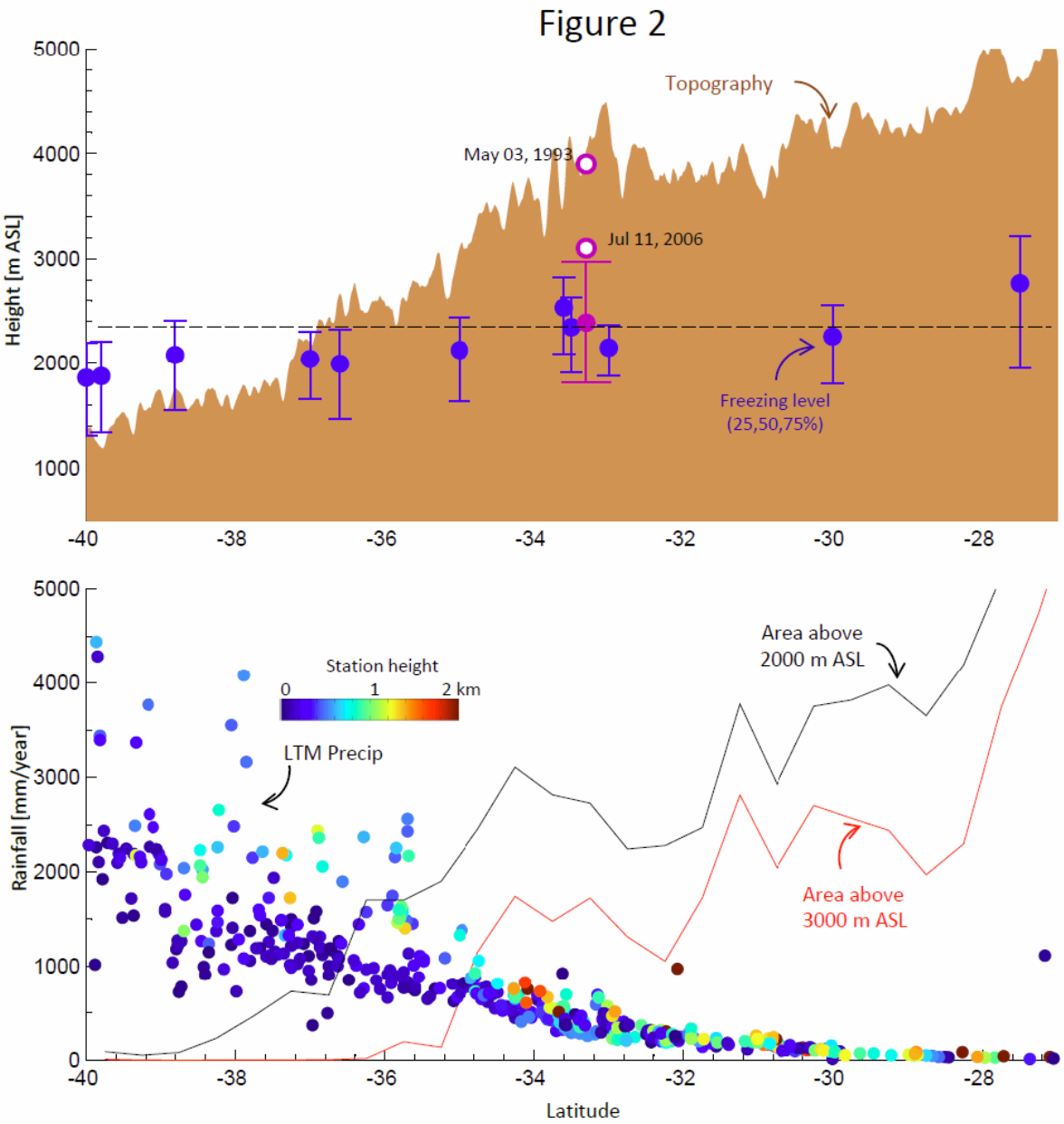

Ground based:
$Hsfc + T_m/\Gamma_{sat}$

Interpolated from Radisonde

Warm and cold winter rainstorms

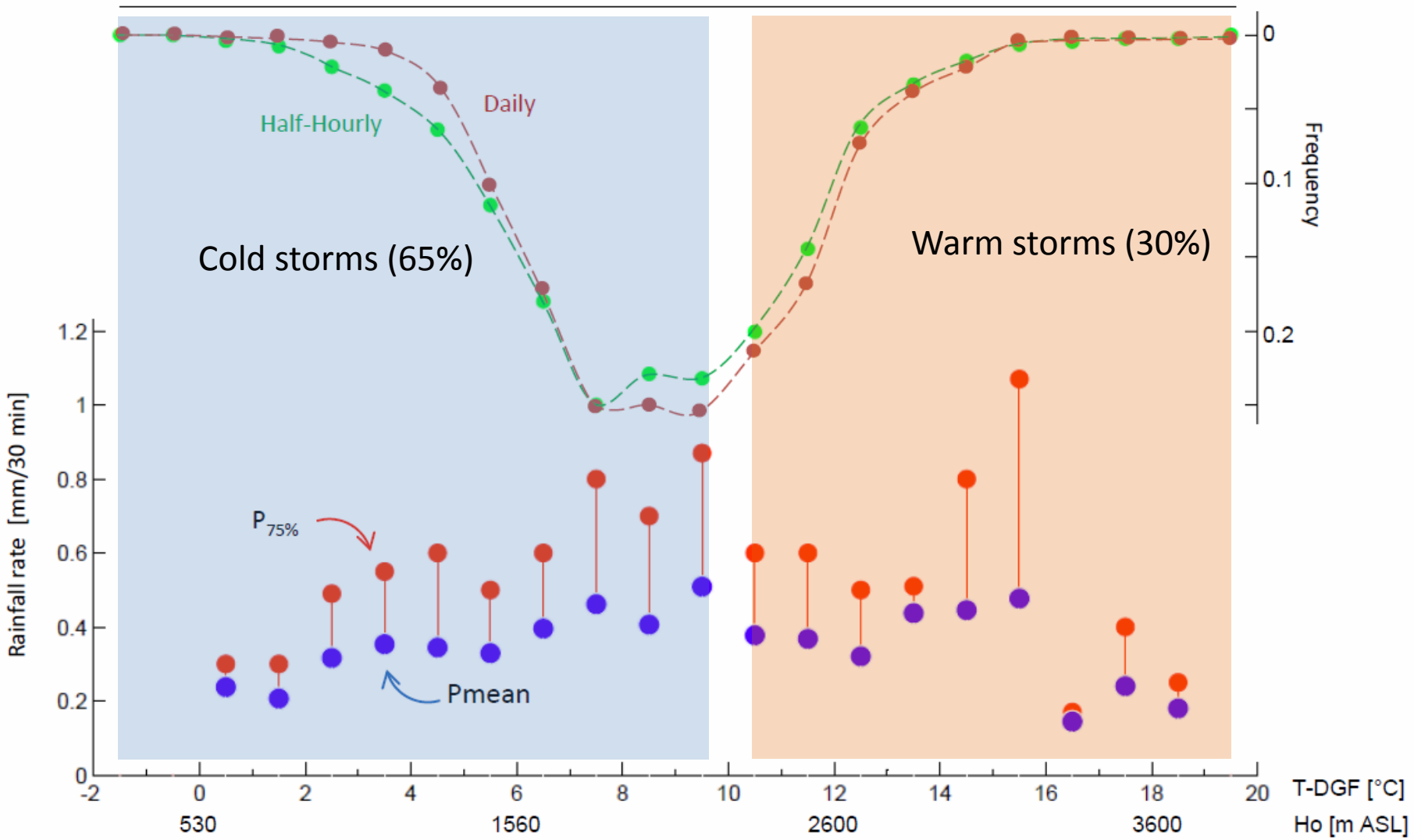

Warm and cold winter rainstorms

Composite local conditions (DGF, 30 min, 2004-11) during cold (44) and warm (22) rainstorms

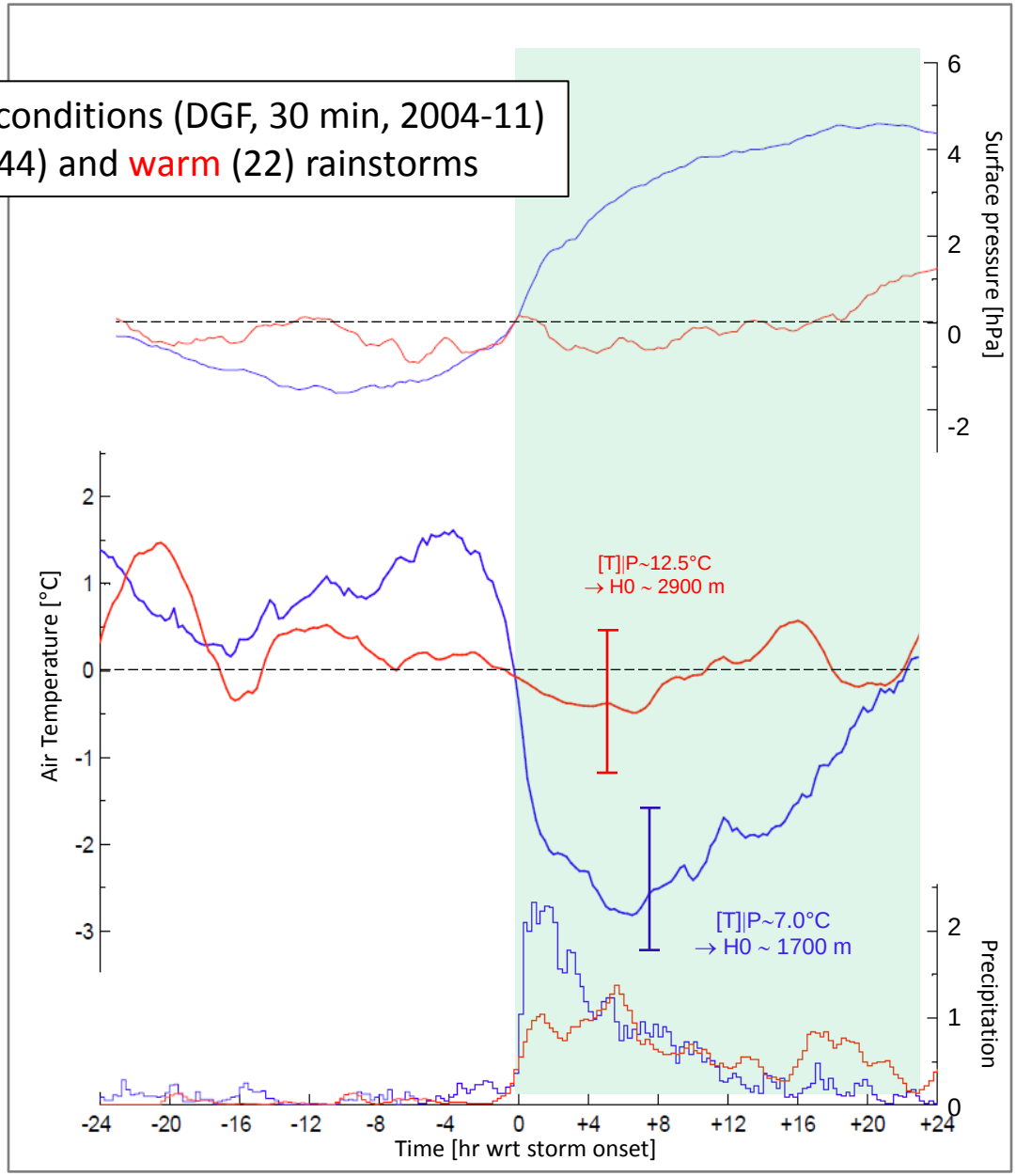

Warm and cold winter rainstorms

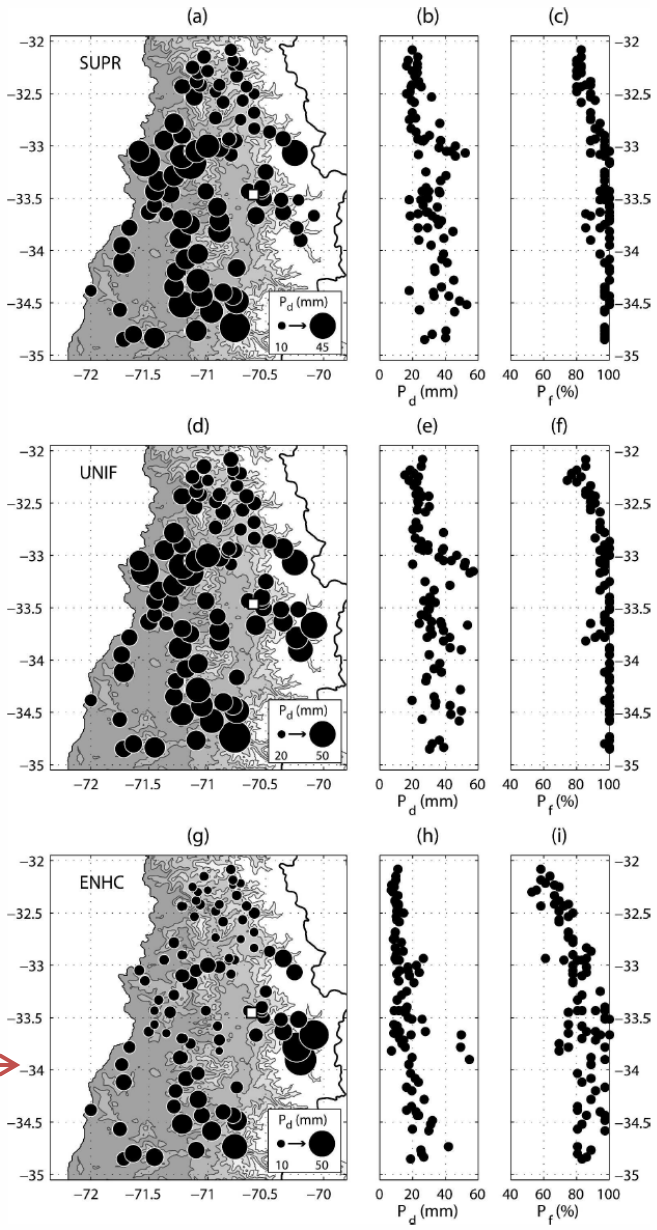

Mountain Enhanced Precipitation Group exhibits warmer conditions (H0 = 2900 m)

Case of study: July 2006

DGF station

Sto. Domingo radiosonde

Sto. Domingo radiosonde

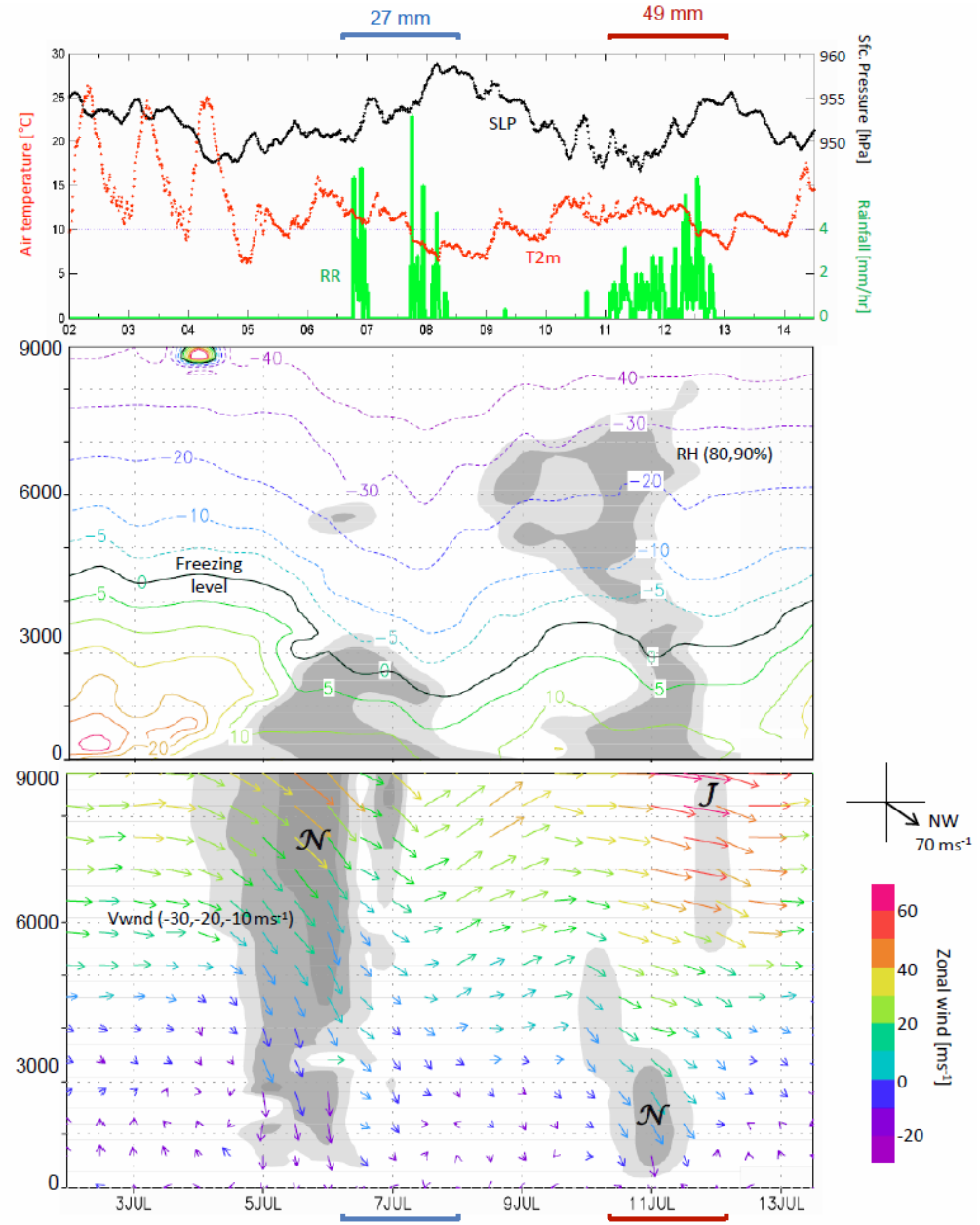

Case of study: July 2006

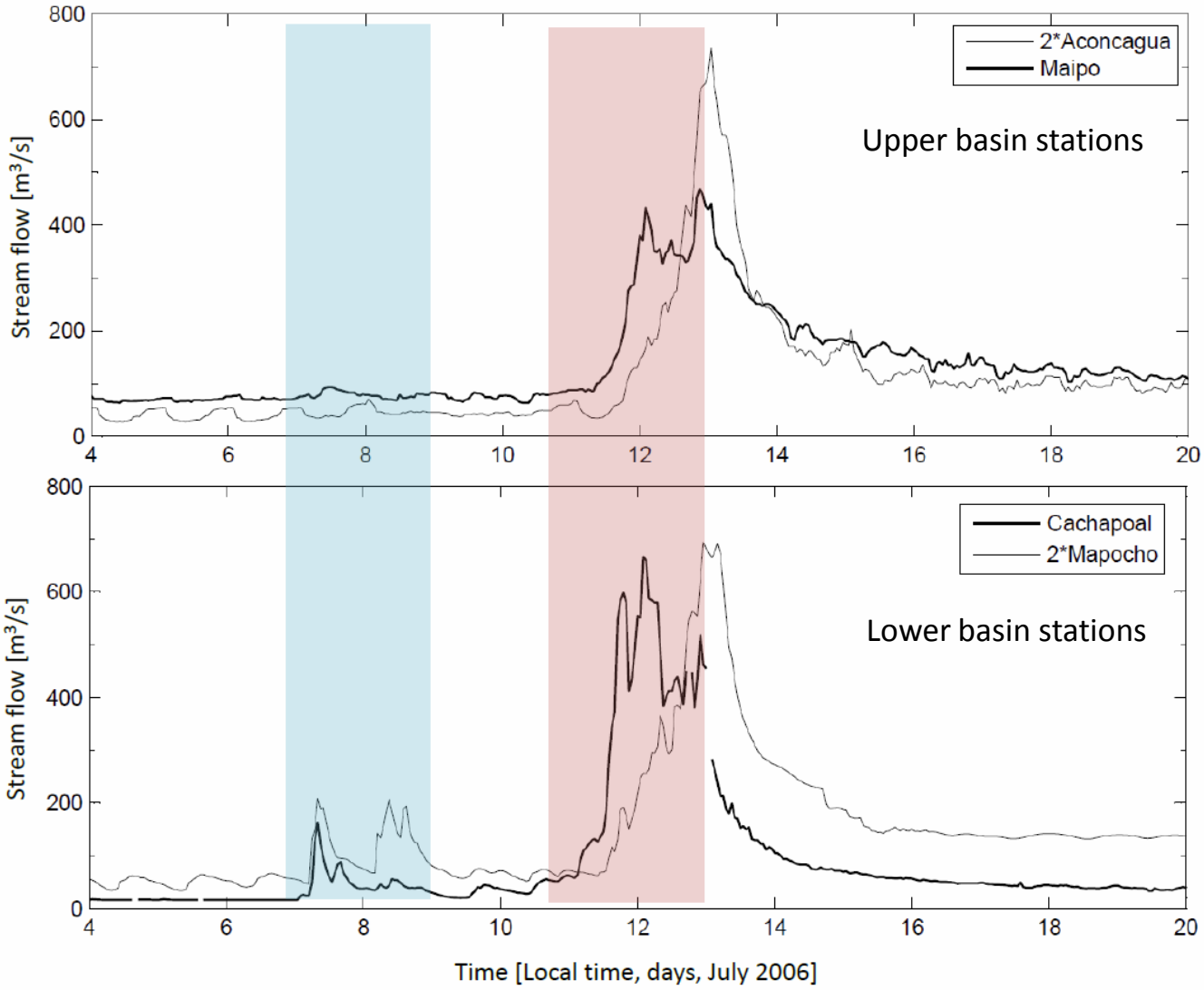

Case of study: July 2006

Wind profiles at Santo Domingo 12Z 11Jul 2006

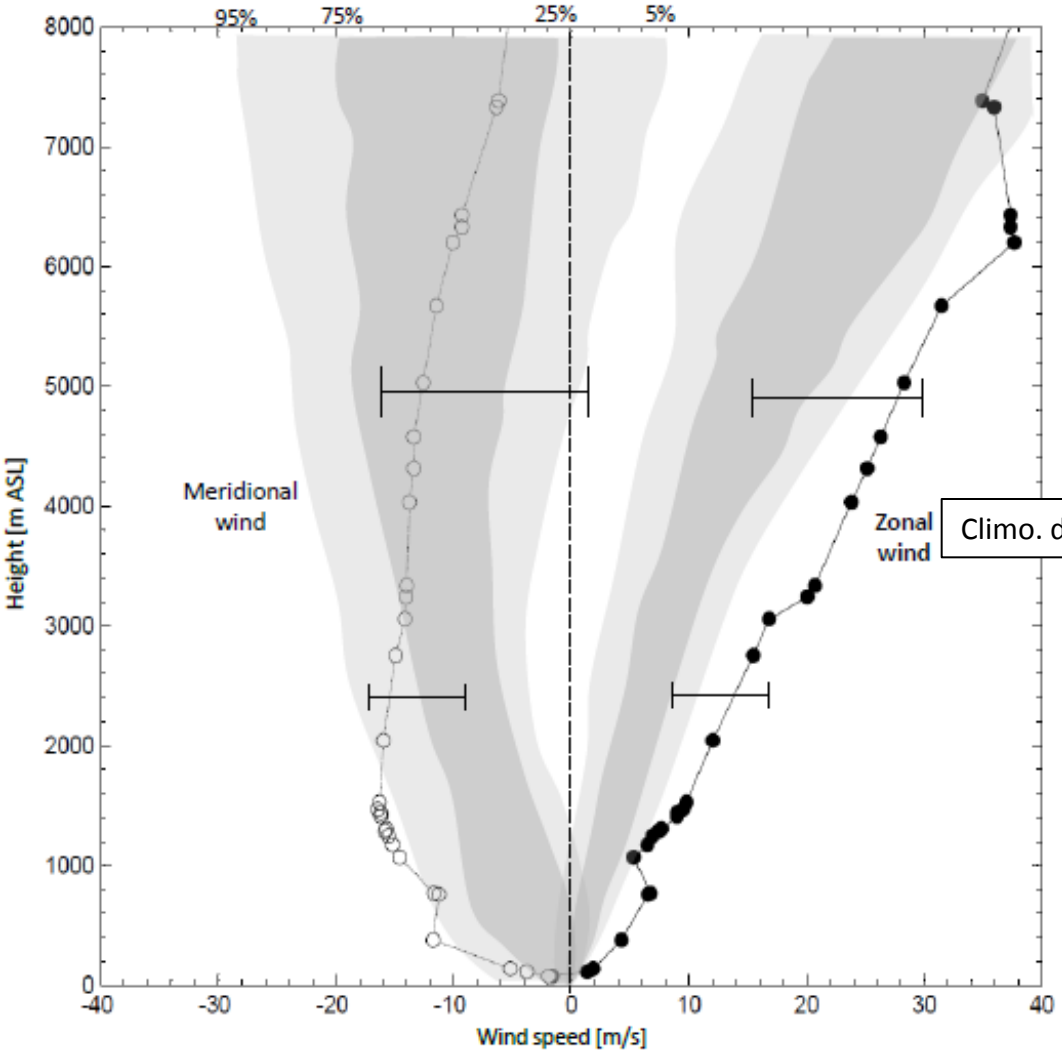

Climo. data from FG2007

Case of study: July 2006

GOES12 IR2 + CFSR 500 hPa winds

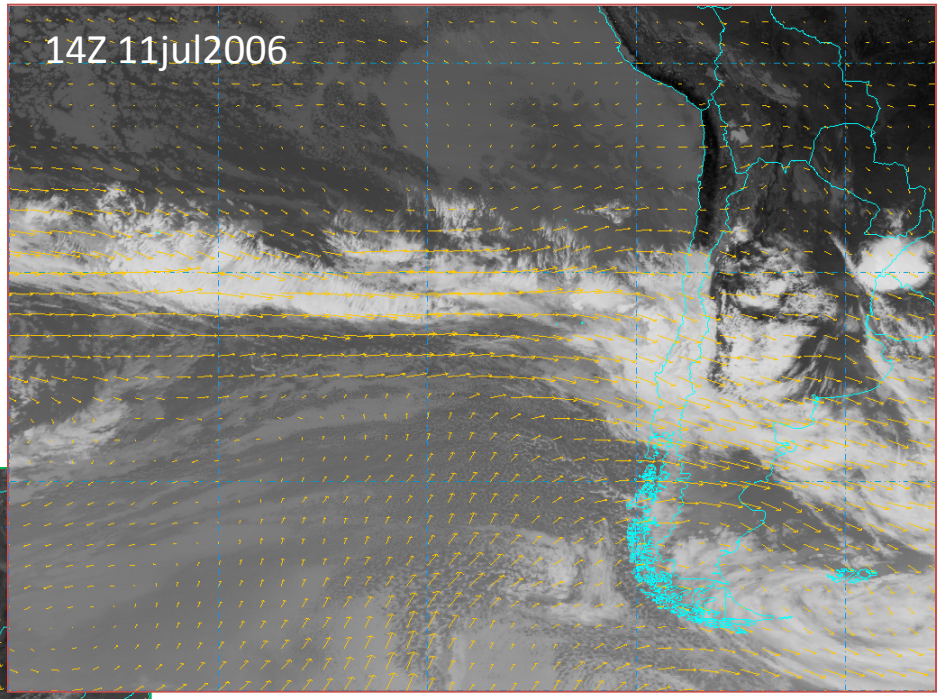

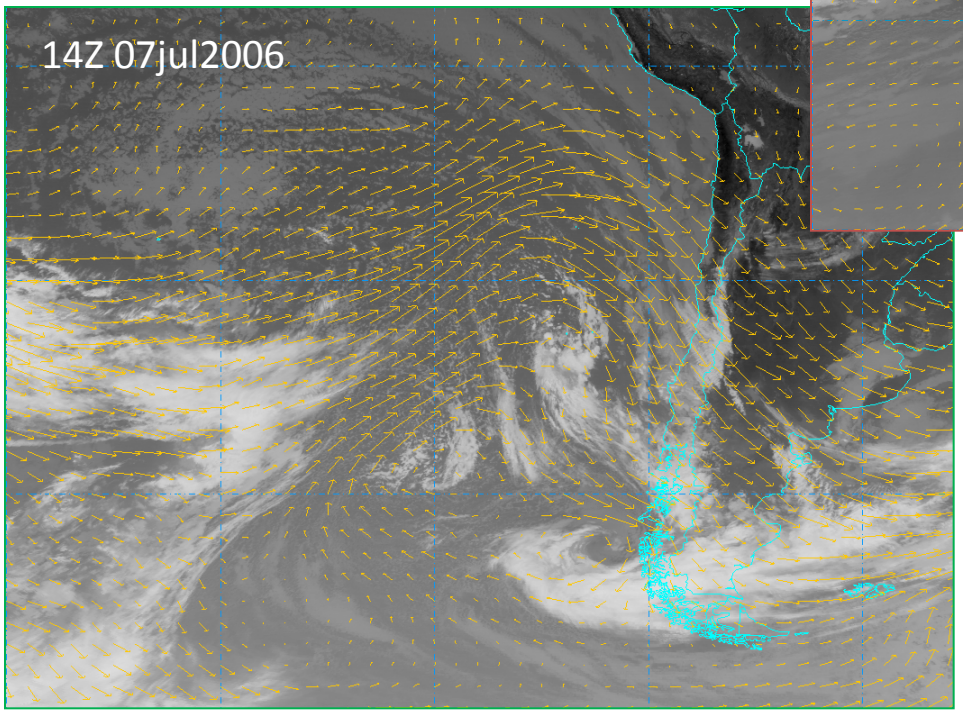

Case of study: July 2006

GOES-12 VIS (1445 UTC) +
TRMM_3B42 daily precip.

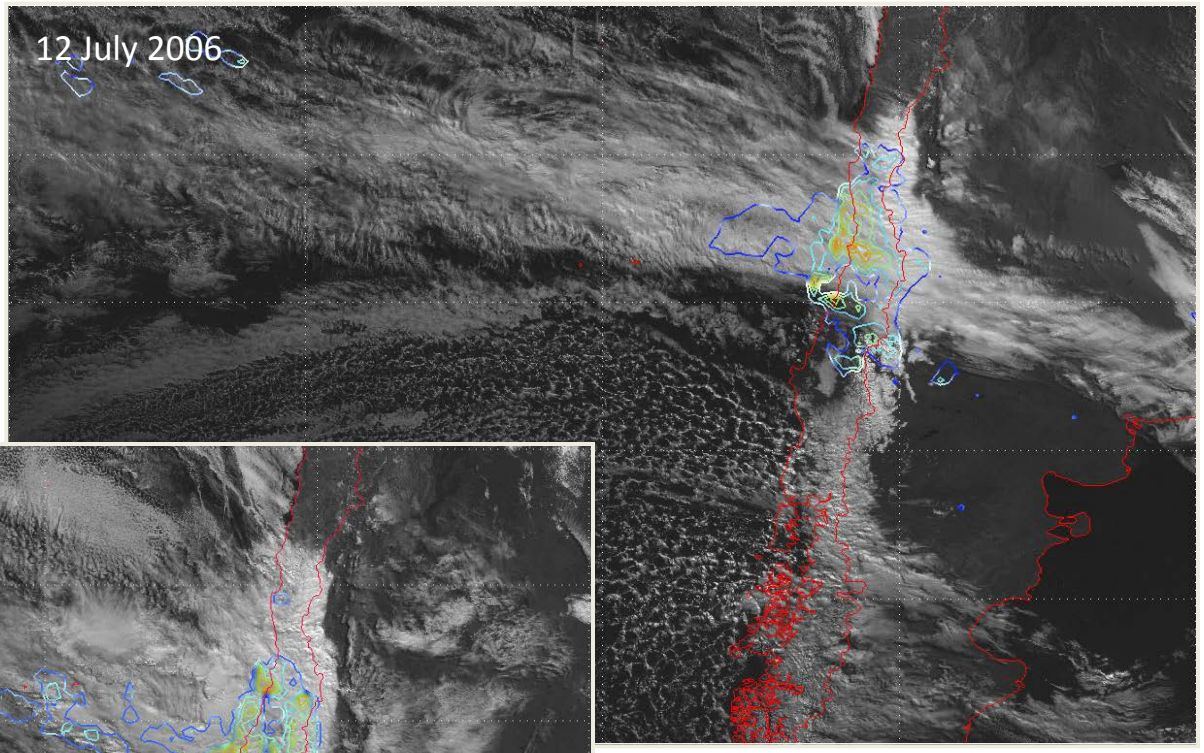

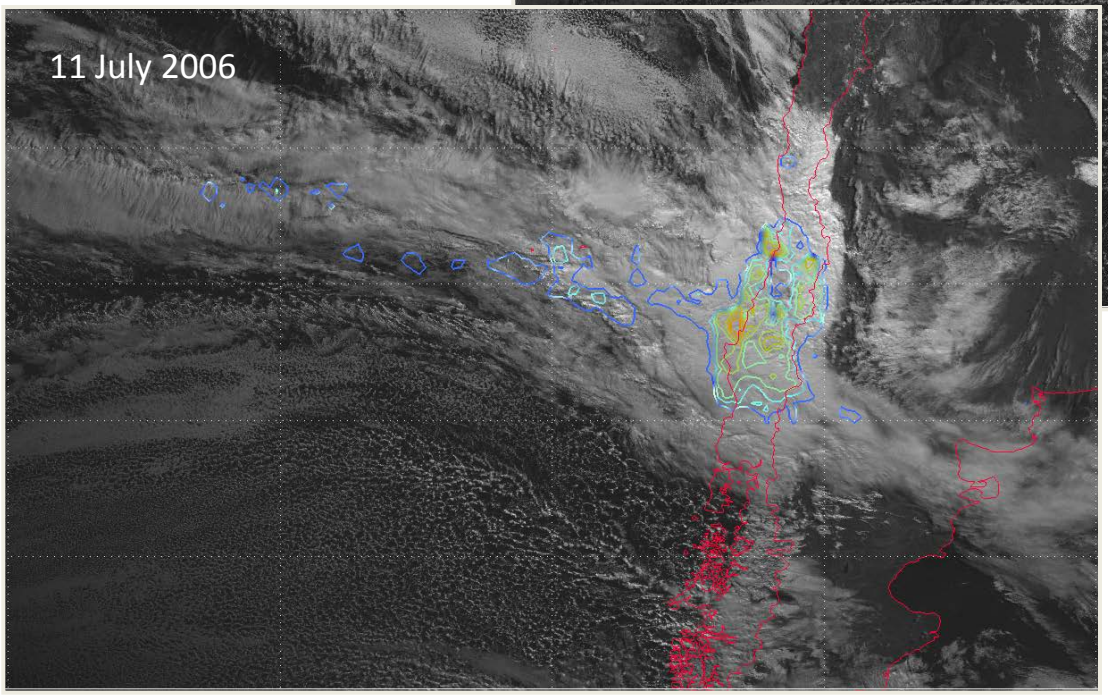

Case of study: July 2006

950 hPa winds, temperature and precipitation 18Z 11 Jul 2006

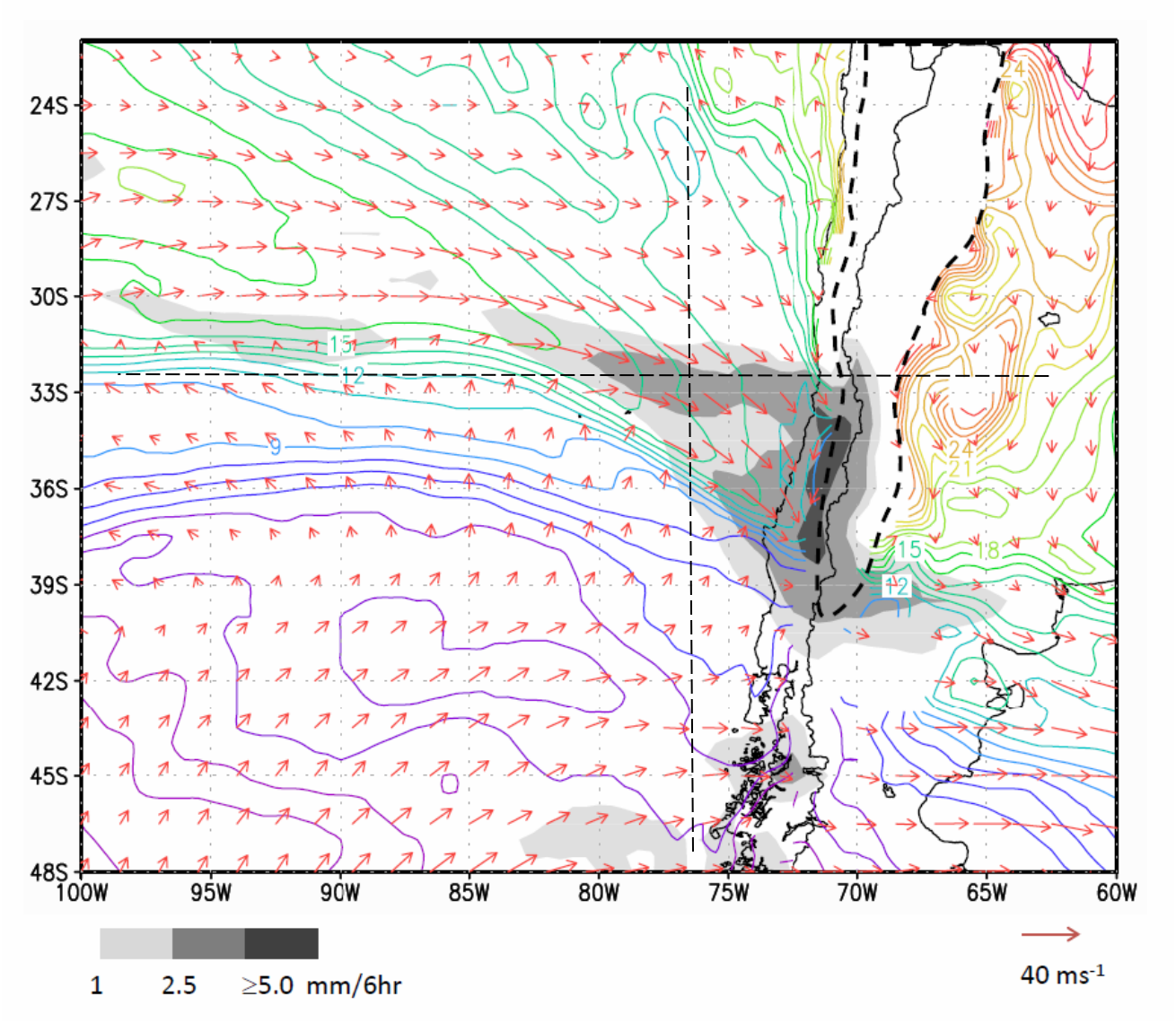

Case of study: July 2006

Lat-height cross sections at 77°W, 18Z 11 Jul 2006

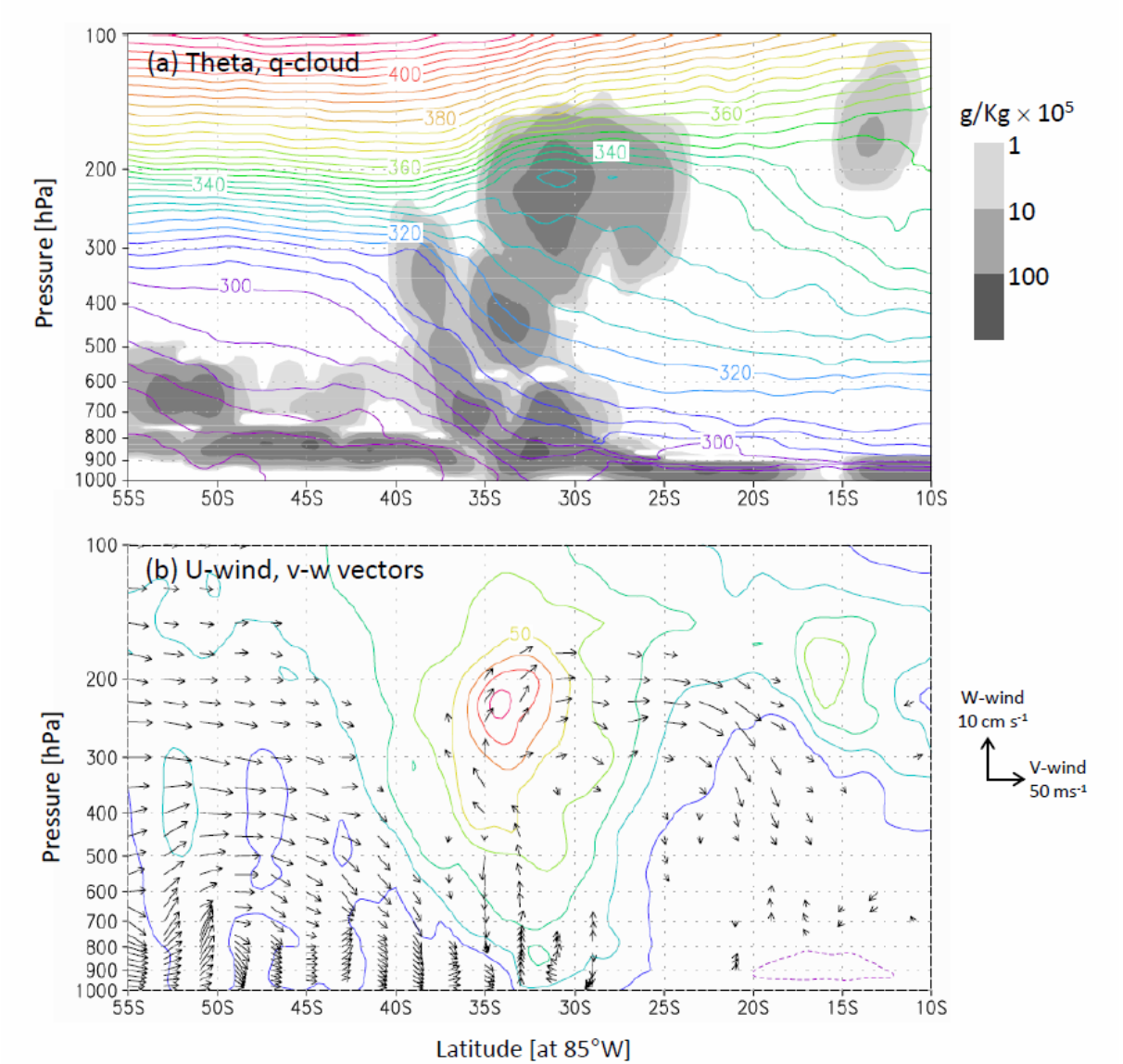

Case of study: July 2006

Lon-height cross sections at 33°W, 18Z 11 Jul 2006

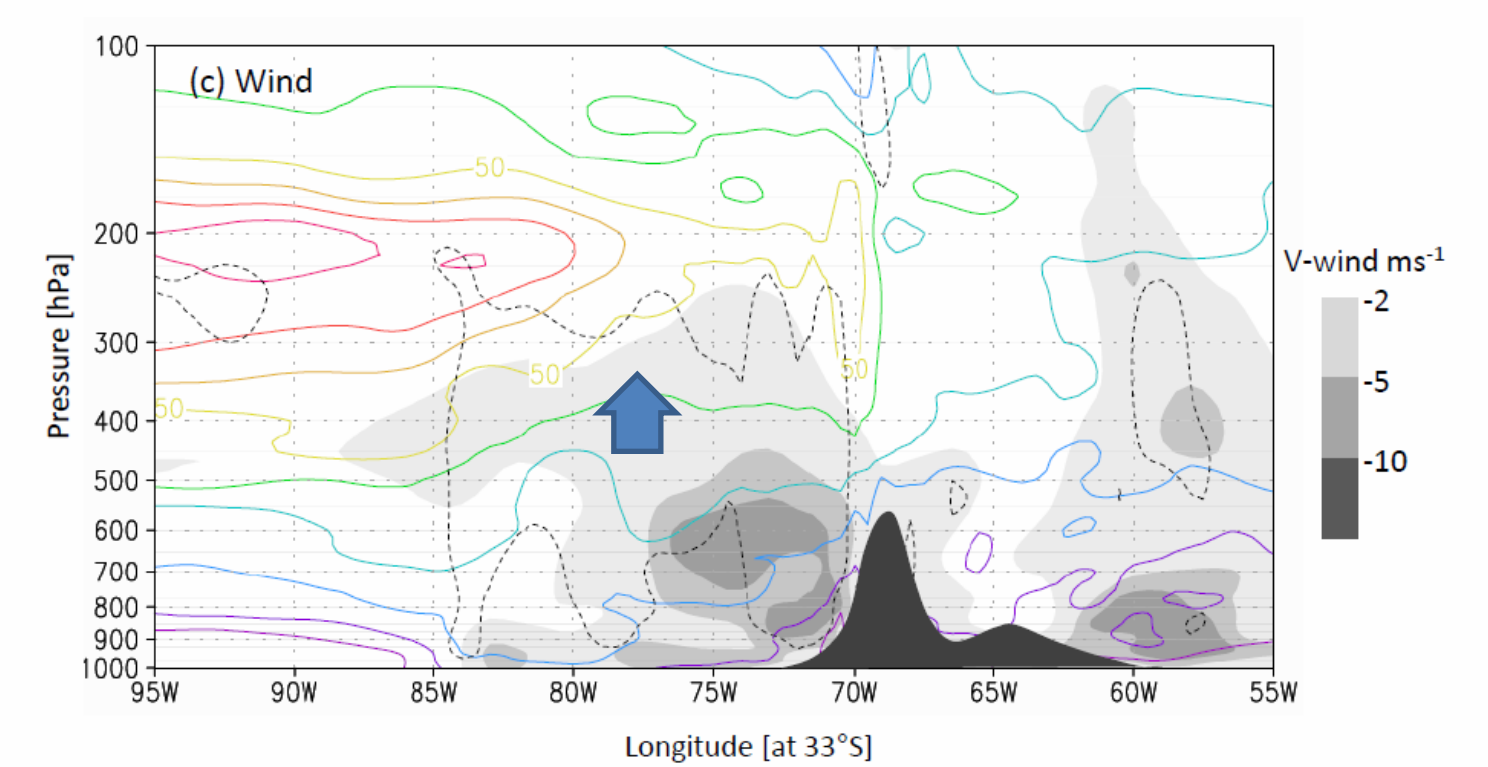

Case of study: July 2006

200 hPa winds, IPW and SLP. 12Z 11 Jul 2006

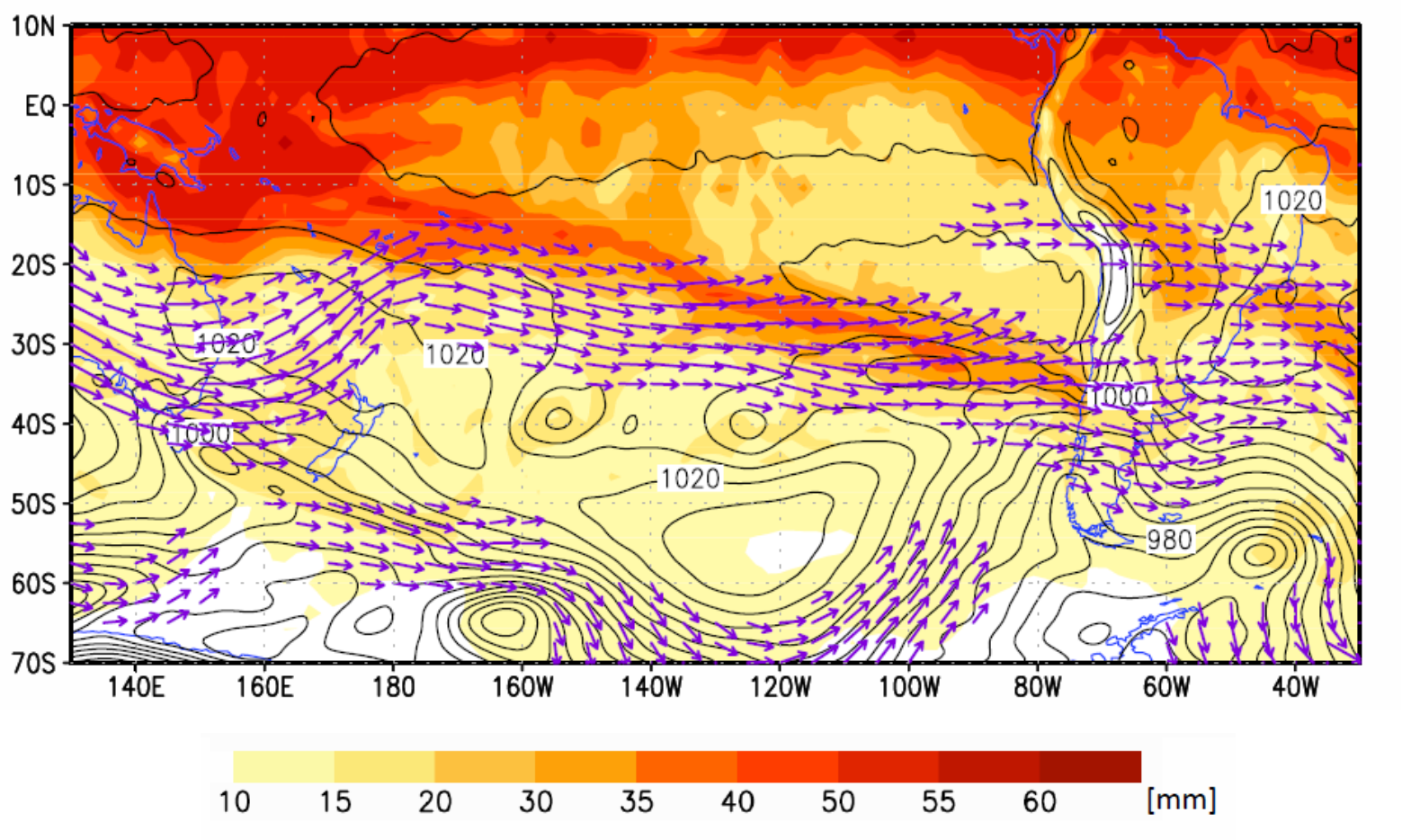

Case of study: July 2006

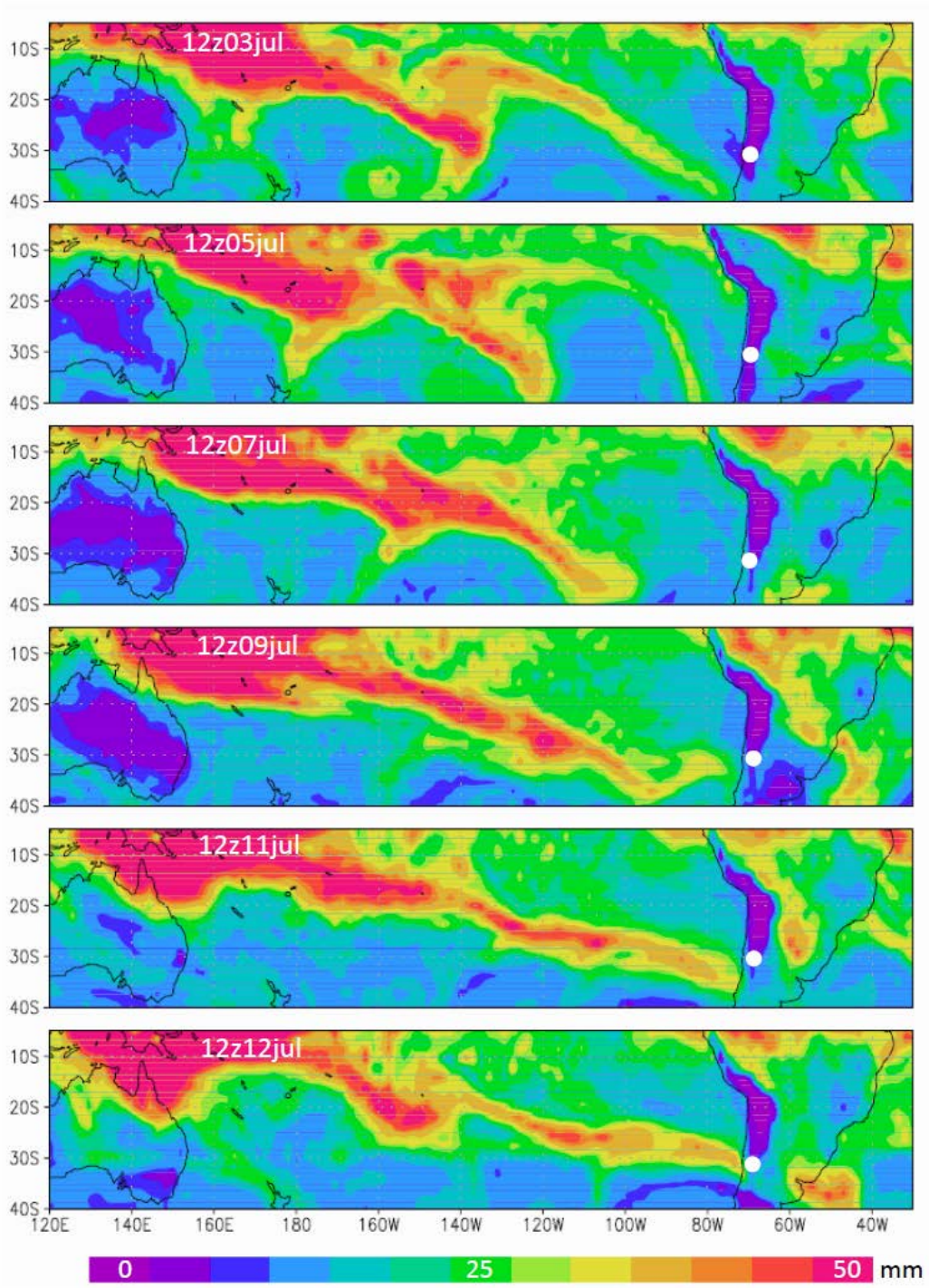

Case of study: July 2006

AM pass 11 Jul 2011

(b) SMI vapor and QS winds

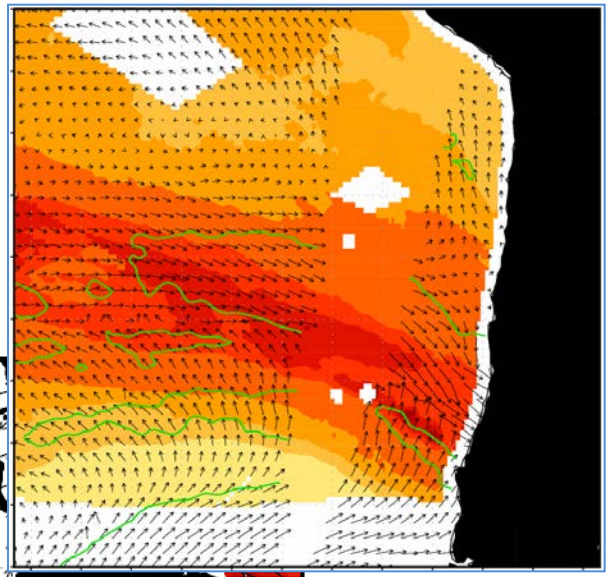

(a) TMI vapor and QS winds

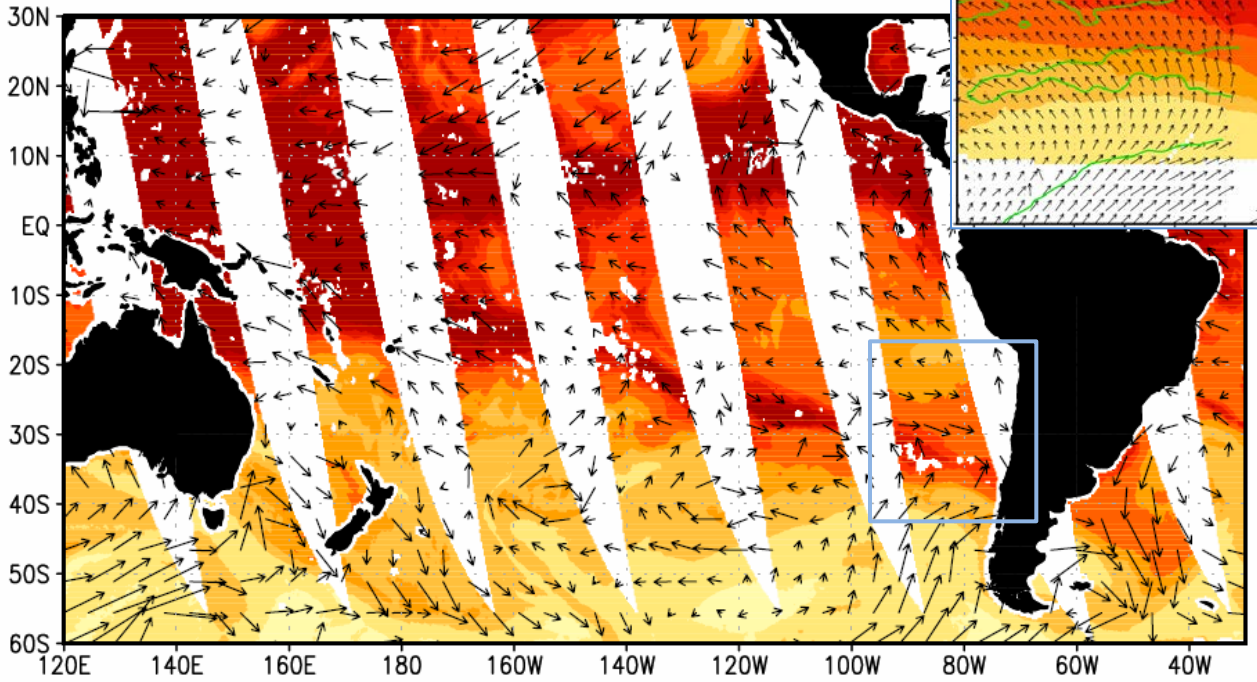

Case of study: July 2006

TRMM_3B42 July 2006

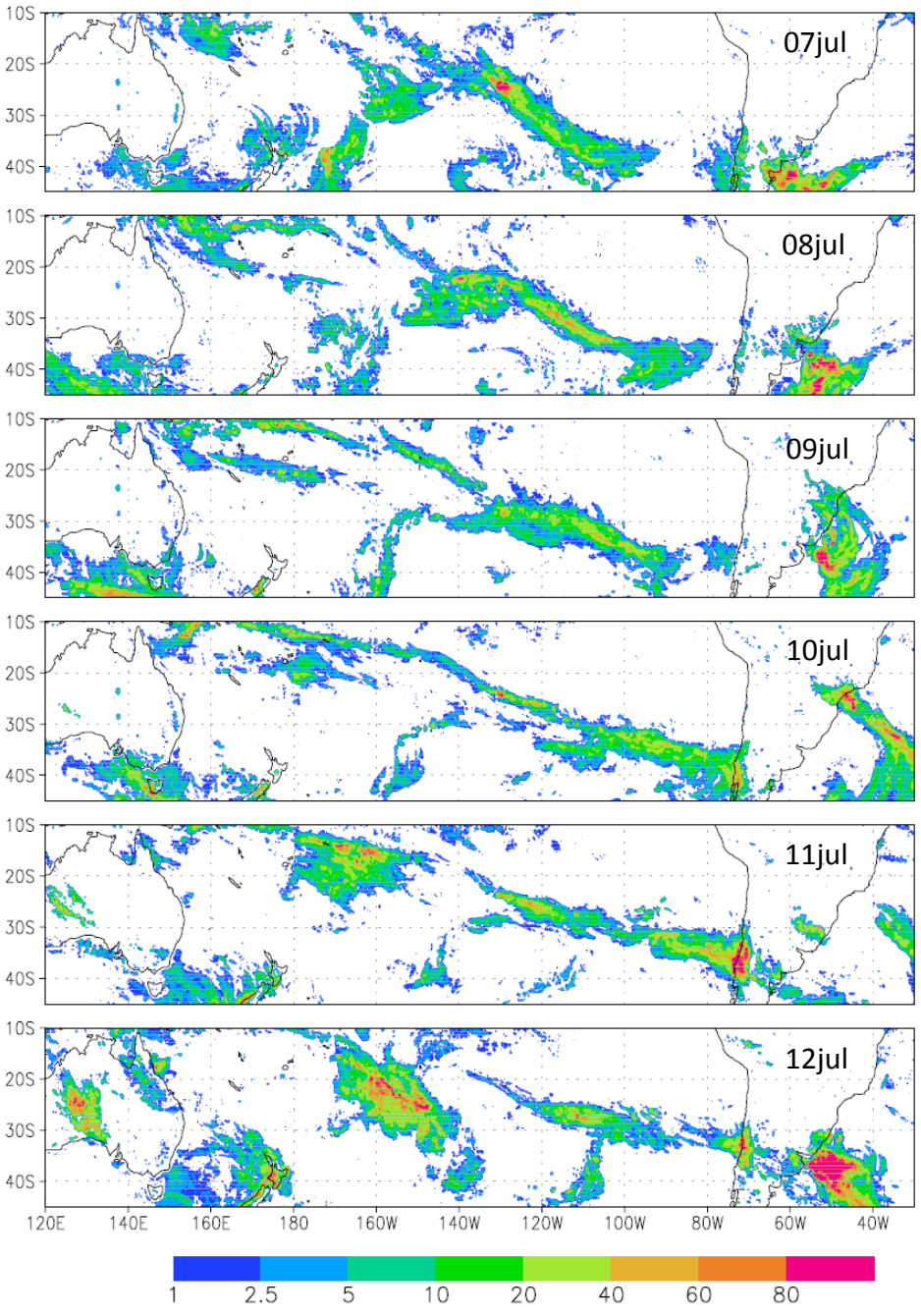

Case of study: July 2006

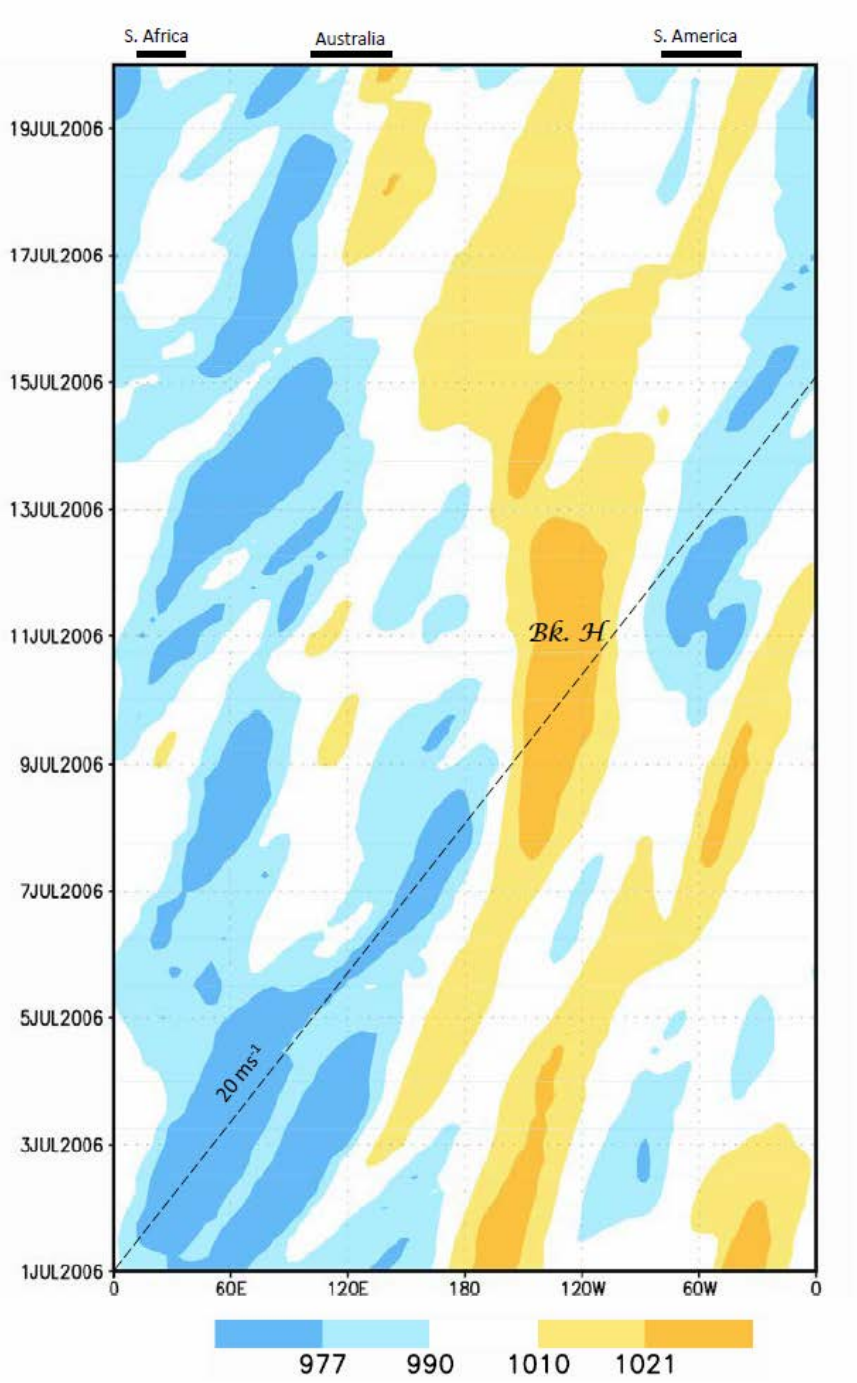

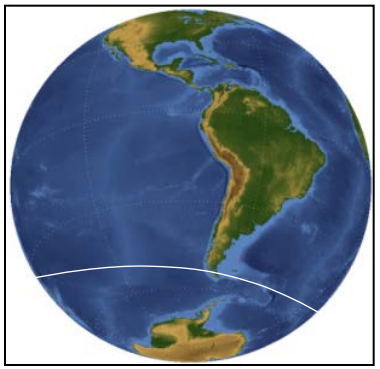

Hovmoller section at 55°S of SLP

Large scale composite analysis: IPW & 200 hPa wind

CFSR averages for cold (44) and warm (22) rainstorms

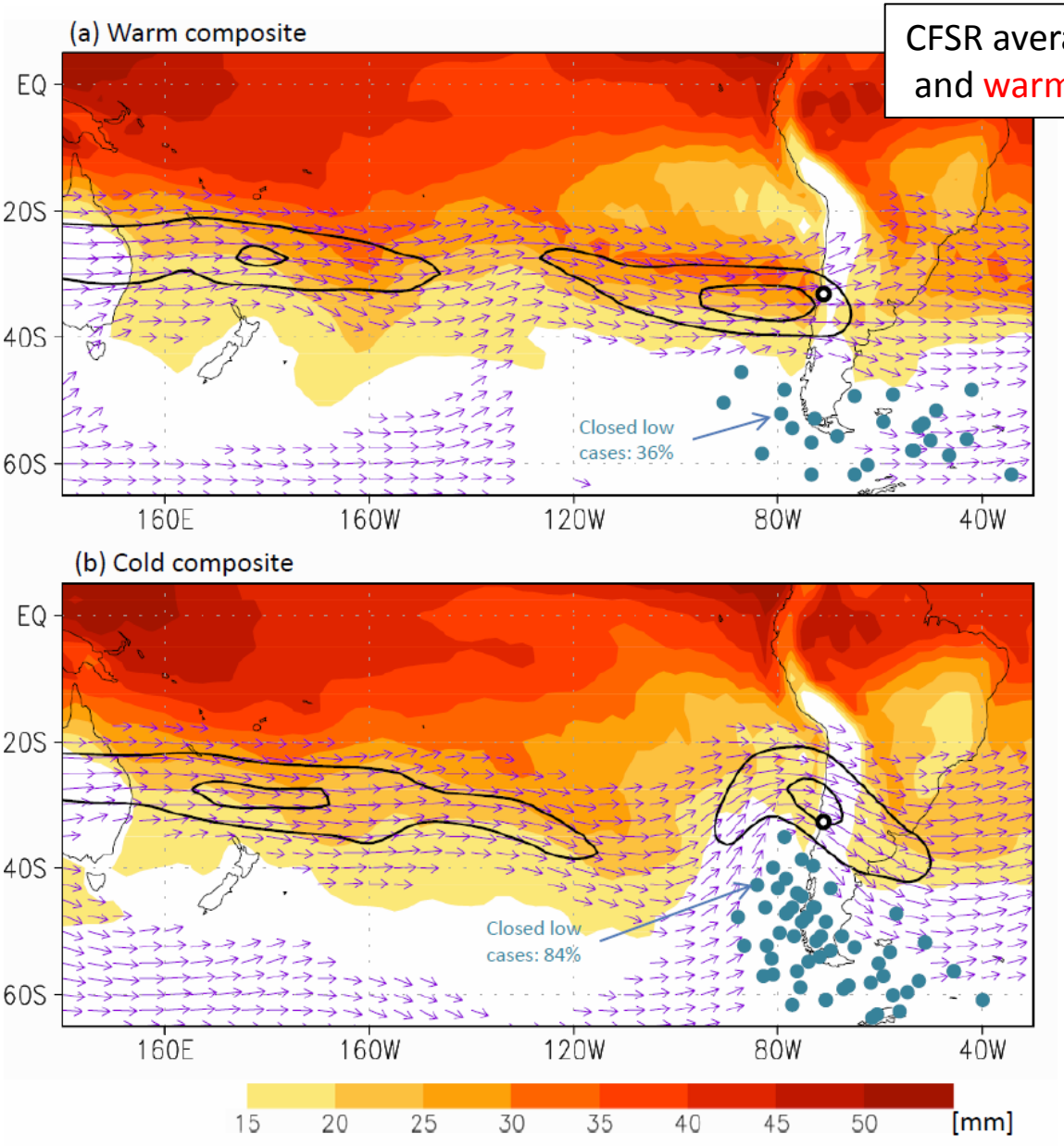

Large scale composite analysis: SLP' & T500'

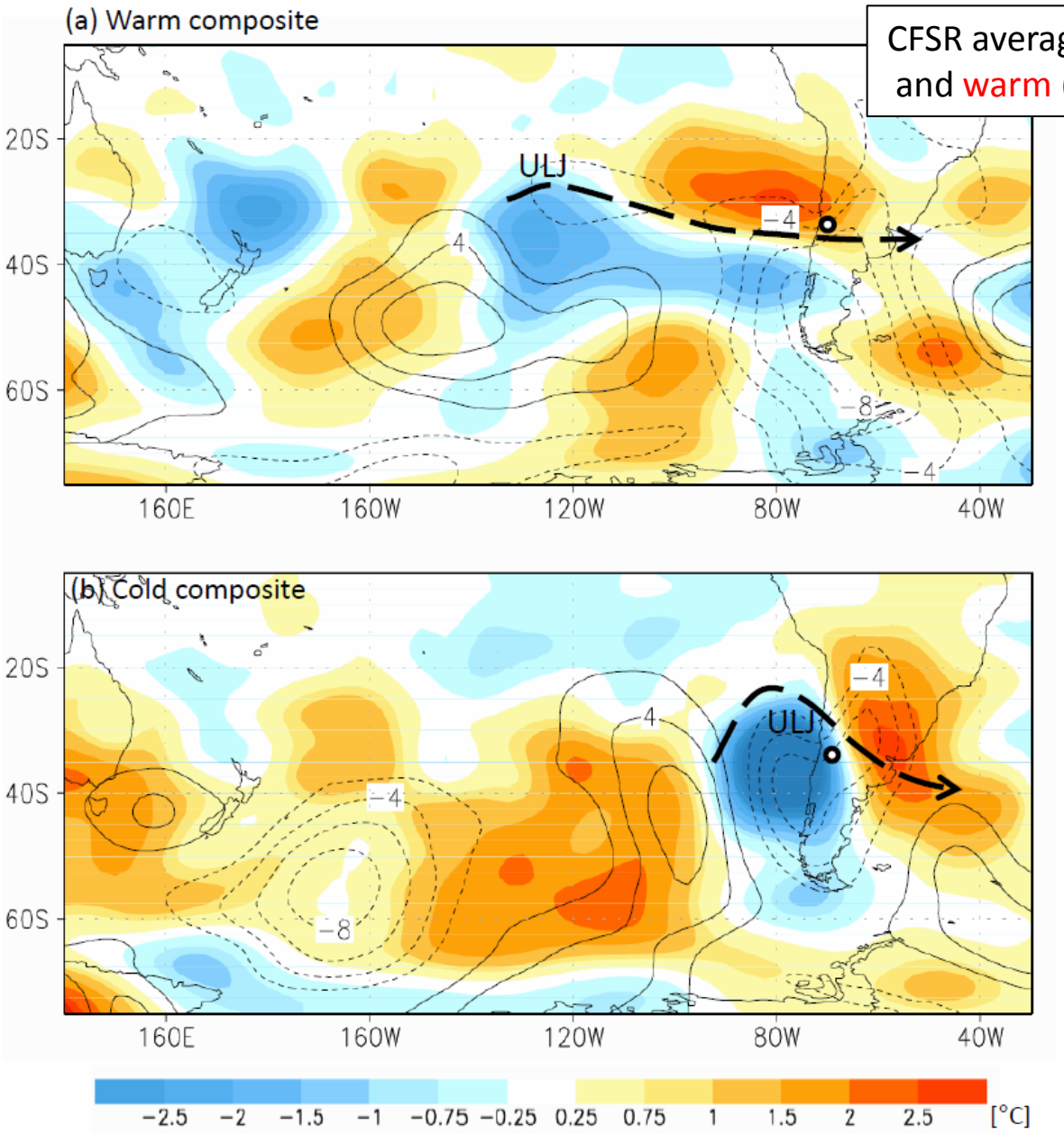

CFSR averages for cold (44) and warm (22) rainstorms

Conceptual Model

- Rainfall at and behind cold front
- H0 < 2500 m ASL
- Prefrontal rainfall up in the Andes
- Well defined baroclinic wave
- Deep cyclone off southern Chile
- NW flow aloft
- Strong topographic blocking
- Northerly low-level jet

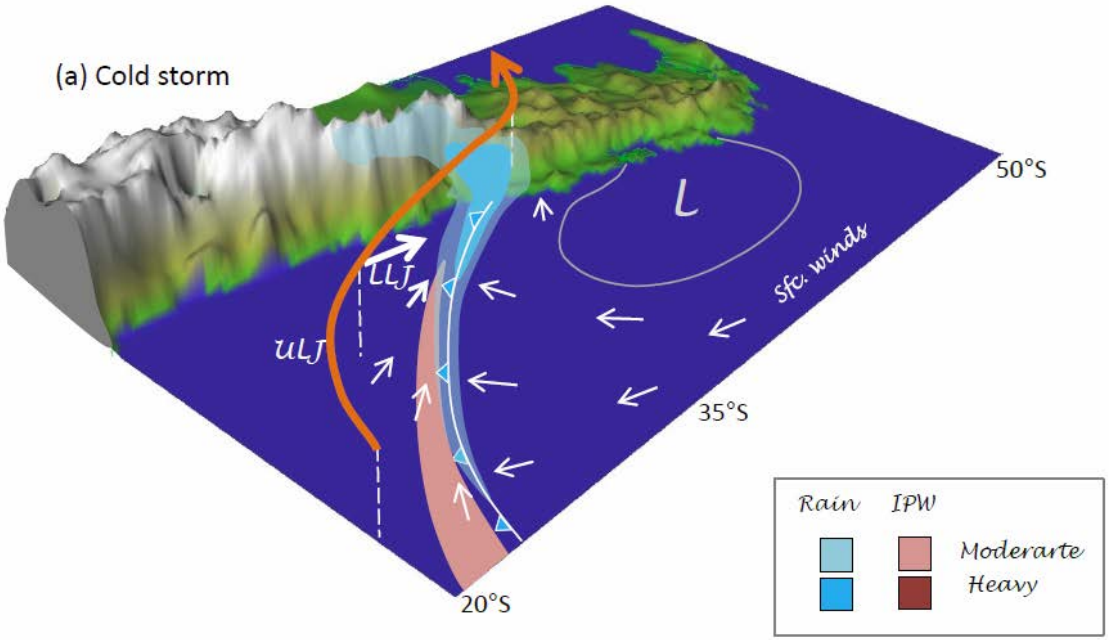

- Rainfall well ahead cold front
- H0 > 2500 m ASL
- Strong W flow aloft
- Conditionally unstable environment
- Reduced topographic blocking
- Wide, deep layer of ascent
- Weak trough farther south
- Blocking anticyclone farther west
- TransPacific zonal jet and troposheric river